Journal of the Serbian Chemical Society
JSCS-info@shd.org.rs • www.shd.org.rs/JSCS
J. Serb. Chem. Soc. *86* (9) 781–793 (2021)
JSCS–5461
Original scientific paper
Published 3 June, 2021

Amide–π interactions in active centres of superoxide dismutase

SRĐAN Đ. STOJANOVIĆ[1], ZORAN Z. PETROVIĆ[2] and MARIO V. ZLATOVIĆ[3]*#

[1]*University of Belgrade-Institute of Chemistry, Technology and Metallurgy, Department of Chemistry, Belgrade, Serbia,* [2]*Faculty of Mathematics, University of Belgrade, Belgrade, Serbia and* [3]*Faculty of Chemistry, University of Belgrade, Belgrade, Serbia*

(Received 21 March, revised 1 June, accepted 2 June 2021)

Abstract: In this work, the influence of amide–π interactions on stability and properties of superoxide dismutase (SOD) active centres was analysed. In the data set of 43 proteins, 5017 amide–π interactions were observed, and every active centre formed averagely about 117 interactions. Most of the interactions belonged to the backbone of proteins. The analysis of the geometry of the amide–π interactions revealed two preferred structures, parallel-displaced and T-shaped structure. The aim of this study was to investigate the energy contribution resulting the from amide–π interactions, which were in the lower range of strong hydrogen bonds. The conservation patterns in the present study indicate that more than half of the residues involved in these interactions are evolutionarily conserved. The stabilization centres for these proteins showed that all residues involved in amide–π interactions were of use in locating one or more of such centres. The results presented in this work can be very useful for the understanding of contribution of amide–π interaction to the stability of SOD active centres.

Keywords: catalytic site; distribution of distances; stabilization of the SOD proteins.

INTRODUCTION

Noncovalent interactions involving aromatic rings (π-stacking, cation–π, anion–π, X–H/π, *etc.*) play vital roles in many chemical and biochemical phenomena.[1–3] The attractive interactions between aromatic groups of amino acids and nearby amides, in polypeptides and proteins (Ar–HN), are weakly polar and have a quadrupole–dipole nature. These interactions can be effectively modelled by the electrostatic interaction between the partial negative charge of an aromatic ring and the partial positive charge of an amide hydrogen.[4] The strength of this

* Corresponding author. E-mail: mario@chem.bg.ac.rs
# Serbian Chemical Society member.
https://doi.org/10.2298/JSC210321042S

interaction in vacuum (–1 to –4 kcal* mol^{-1}) is almost comparable with that of a conventional hydrogen bond (–2 to –7 kcal mol^{-1}).[4–6] Therefore, the function and the formation of Ar–NH interactions in the protein structure are heavily dependent on the conformational consequences of stronger forces, such as the conventional hydrogen bond. On the basis of the location of the NH group in a polypeptide, the interactions between an aromatic ring and NH can be characterized as either Ar–NH(side chain) or Ar–NH(backbone). Furthermore, as the protein backbone is less flexible than the amino acid side chains, it should be simpler to target amide stacking interactions through the structure-based drug design.[7] Additionally, the large number of intra-protein hydrogen bonds involving backbone amides means that the π-face of these functional groups is typically more accessible for the interactions with ligands.[8]

The importance of aromatic interactions in proteins were pointed out first by Burley and Petsko,[9] in their work on interaction between phenylalanine residues. Studies by Burley and Petsko suggested the involvement of Ar–NH interactions in the stabilization of protein tertiary structures, on the basis of their spatial distribution.[10,11] Further investigations by various research groups established the role of these interactions in the ligand recognition and the stabilization of secondary structures, mainly β-sheets and helix termini.[12–15] The Diederich lab has taken the lead in increasing our understanding of these interactions and the knowledge gained from this structure-activity relationship study and the detection of the binding mode has been continuing to inspire their use in rational design.[16–22]

The planar residues, such as His, Tyr, Asp, Arg, Pro, *etc.* are usually playing an important role at the catalytic and binding sites.[23] Furthermore, the amide groups are abundant in protein binding sites, either as part of the backbone or asparagine and/or glutamine side chains. Therefore, to explain the role of amide––π interactions in the secondary and the local structures of superoxide dismutase, as well as to improve the prediction of the amide–π interaction, 43 protein structures for the amide–π interactions between the aromatic ring of His, Phe, Trp, and Tyr and the amide group of any residue in superoxide dismutase (SOD) active centres were analysed.

EXPERIMENTAL

Dataset

For this study, the Protein Data Bank (PDB) October 5th, 2020, list of 173,420 structures was used.[24] The selection criteria for the superoxide dismutase to be included in the dataset were as follows: 1) the crystal structures of proteins containing E.C. Number 1.15.1.1 (superoxide dismutase) with metal were accepted; 2) the theoretical model structures and the NMR structures were not included (these structures were not accepted as it was difficult to define the accuracy of the ensemble of structures in terms of displacement, that was directly comparable to the X-ray diffraction studies); 3) the only crystal structures with the resolution of 2.0 Å

* 1 kcal = 4184 J

or better and a crystallographic *R*-factor of 25.0 % or lower were accepted; 4) only representatives at 30 % sequence identity were included. After assembling the dataset, several structures containing ligands and mutant amino acids were rejected, thus leaving 43 proteins that were actually used as the dataset in our analysis. The hydrogen atoms were added and optimized, where needed, using the program Reduce,[25] with default settings. Reduce software adds hydrogen atoms to protein and/or DNA structures in standardized geometry, optimizing them to the orientations of OH, SH, NH_3^+, Met methyls, Asn and Gln sidechain amides, and His rings. The software determines the best hydrogen positions by selecting the best overall score from all of the possible combinations, taking into the account individual scores assigned for each individual residue and for groups containing movable protons partitioned in closed sets of local interacting networks. The PDB IDs of selected structures (protein chains) are as follows: 1ar5:A, 1cbj:A, 1d5n:A, 1hl5:A, 1ids:A, 1isa:A, 1kkc:A, 1my6:A, 1qnn:A, 1srd:A, 1to4:A, 1unf:X, 1xre:A, 1xuq:A, 1y67:A, 1yai:A, 1yso:A, 2aqn:A, 2cw2:A, 2goj:A, 2rcv:A, 2w7w:A, 3ak2:A, 3ce1:A, 3dc6:A, 3evk:A, 3f7l:A, 3h1s:A, 3js4:A, 3lio:A, 3lsu:A, 3mds:A, 3pu7:A, 3tqj:A, 4br6:A, 4c7u:A, 4f2n:A, 4ffk:A, 4yet:A, 5a9g:A, 5vf9:A, 6bej:A, and 6gsc:A.

Amide–π interaction analysis

For the selection of the protein structures having various types of amide–π interactions, Discovery Studio Visualizer 2020 was used,[26] with some specific criteria and geometrical feature settings. Amide–π stacked interactions occur between an amide group and a π ring if the following criteria are satisfied (Fig. 1): 1) the distance between the centroid of the amide group and the π rings falls within the π–π centroid (max dist, R_{cen}; 7 Å); 2) an atom from the each group should be within the π–π closest atom (max dist, R_{clo}; 7 Å); 3) the angle θ between the normal of one or both groups and the centroid–centroid vector must be between 0° and ± the stacked π–amide theta angle cut-off distance, and the angle γ between the normal to each must be between 0° and ± the stacked π–amide gamma angle cut-off. The centroid of amide group plane was taken as the midpoint of C and N atoms. Compared to the criteria applied in the studies of small molecules found in the Cambridge Structural Database (CSD) these criteria were a bit more relaxed. The slightly looser criteria were selected because the structural variations in crystal structures of proteins are generally larger than in crystal structures of small molecules. The earlier publications confirmed π interactions as long-range interactions, having notable binding forces even at intermolecular distances of 7 Å.[27-29]

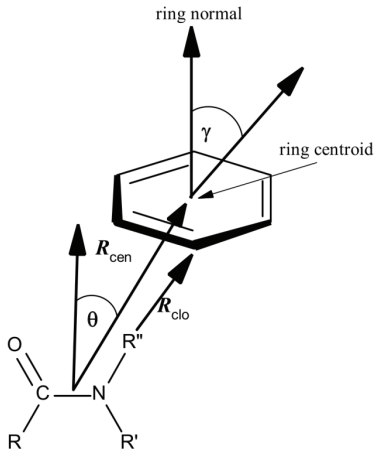

Fig. 1. Parameters for amide–π interactions: (R_{cen}) the distance between the centroid of the amide group and the π ring; (R_{clo}) the distance between π–π closest atoms from each group; (θ) the angle between the amide–centroid vector and a chosen vector on the principle axis of the aromatic ring; and (γ) the angle between the normal of each ring.

Computation of amide–π interaction energy

In order to apply *ab initio* methods in determining the energies of amide–π pairs on the desired level of theory, with the sufficient level of accuracy and still in satisfactory time frame, the calculations were performed on structurally reduced model systems.[29] We used formamide (**1**) as mimics for amide groups. Phenylalanine was simplified to methylbenzene (**2**), histidine to 5-methyl-1*H*-imidazole (**3**), while tryptophan and tyrosine were reduced to 3-methyl-1*H*-indole (**4**) and 4-methyphenol (**5**), respectively (Fig. 2).

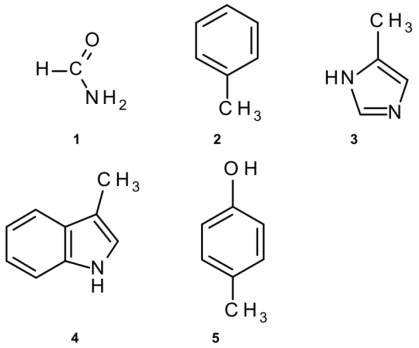

Fig. 2. Structurally reduced structures used for calculations of amide–π interaction energy: **1** instead of amide; **2** instead of Phe; **3** instead of His; **4** instead of Trp; **5** instead of Tyr.

The use of a reduced model systems in calculations of specific intramolecular interaction in large systems is a well-known and already proved methodology,[30] producing the results which are accurate enough, but significantly reducing the computation times and the strength needed for them. Larger models, like whole amino acids, or parts of protein chain, will complicate the calculations unnecessarily and can probably even bring in errors. Numerous interactions mechanisms are possible in a larger protein structure, and a single binding energy computation cannot always determine the accurate result, meaning which of these are present and to what amount they contribute to overall stabilization. As a result, separating the involvement of the amide–π interaction from the interacting pair, based on their energies residues involved in other noncovalent interactions, is difficult.

Ab initio calculations were performed using Jaguar from Schrödinger Suite 2018-1,[31] using local Møller–Plesset second-order method (LMP2) method with triple zeta Dunning's correlation consistent basis set[32] and ++ diffuse functions.[33] All calculations were performed in vacuum. The LMP2 method applied to the study of amide–π interactions, showed to be considerably faster than the MP2 method, while the calculated the interaction energies and the equilibrium distances were almost identical for both methods.[34] Several authors found that LMP2 represents an excellent method for calculation of interaction energies in proteins.[35,36] Sometimes calculation results can be influenced largely by BSSE, so taking it into the account is mandatory, therefore the calculation times are longer. The local correlation methods (such as LMP2) not only reduce the cost of the calculations, but the local Møller–Plesset second-order method LMP2 is well known for reducing the intramolecular basis set superposition error (BSSE).[37-39]

Geometries of the interacting structures were optimized and their single point energies calculated using LMP2/cc-pVTZ(-f)++ level of theory. The optimized geometries of molecules were placed to match the corresponding complexes by superimposing heavy atoms onto their respective coordinates, taken from the crystal structures, and the energies of dimeric structures produced which were calculated way.

The amide–π interaction energies in dimers (amide–π pairs) were calculated as the difference between the energy of the complex and the sum of the energies of the monomers in their optimized geometries.

Computation of stabilization centres

The stabilization centres (SC) are defined as the clusters of residues which make cooperative, noncovalent long-range interactions.[40] Measured as individual interactions, the stabilization forces resulting from noncovalent long-range interactions are not very strong, but since they are cooperative by their nature they could play an important role in maintaining the overall stability of protein structures in regions where they act in a group (SC). In order to analyse SC of interaction-forming residues, we used the SCide program.[41] The criteria SCide uses for determining SC are as follows: 1) two residues are in contact if there is, at least, one heavy atom–atom distance smaller than the sum of their van der Waals radii plus 1 Å; 2) a contact is recognized as "long-range" interaction if the interacting residues are, at least, ten amino acids apart; 3) two residues form a stabilization centres if they are in long-range interaction and if it is possible to select one–one residue from both flanking tetrapeptides of these two residues that make, at least, seven contacts between these two triplets.[41]

Computation of conservation of amino acid residues

The conservation of the amino acid residues in each protein was computed using the ConSurf server.[42] This server computes the conservation based on the comparison of the sequence of given PDB chain with the proteins deposited in Swiss–Prot database[43] and finds the ones that are homologous to the PDB sequence. The number of PSI–BLAST iterations and the *E*-value cut-off used in all similarity searches were 1 and 0.001, respectively. All the sequences, that were evolutionary related to each one of the proteins in the dataset, were used in the subsequent multiple alignments. Based on these protein sequence alignments, the residues were classified into nine categories, from highly variable to highly conserved. Residues with a score of 1 are considered to be highly variable and residues with a score of 9 are considered to be highly conserved.

RESULTS AND DISCUSSION

A detailed analysis of the amide–π interactions in SOD involving backbone and side-chain groups, which are fully or partially in the active centres, is presented here. Our study was focused on the active centres, thus the amide–π interactions within the rest of the protein structures were not considered. In the dataset, there are 173,420 proteins. Using the geometrical criteria described in the Experimental section, we found 43 protein crystal structures. The analyzed protein set contains 5017 amide–π interactions. Thus, on average, every active centre forms 117 interactions. The quantification of such interactions is of great importance for a rational approach to biological systems including protein structure and function, as well as for the further development of drug design processes.

Distribution of amide–π interactions

The occurrence of different types of amide–π interactions found in the present dataset is presented in Table I. We noticed that almost all of the interactions were of backbone amide–π interactions type. These kind of interactions stabilize

tertiary and local structures and strengthen protein–ligand interactions.[44] However, although all protein structures contain side-chain amide groups (Asn, Gln and Arg) in the active centres, in our dataset those accounted for only 0.04 % of all amide–π interactions. It has been found that among the aromatic residues, the most efficient π-acceptor is the imidazole group of the histidine residue, followed by the indole group of tryptophan and the phenol moiety of tyrosine. This might be because, of all the aromatic amino acids, His occurs most frequently in both coordination spheres of active centres.[29]

TABLE I. Frequency of occurrence of amide–π interaction-forming residues in active centres of superoxide dismutase

Residue	Amide		π	
	Number[a]	Occurrence, %[b]	Number	Occurrence, %
Backbone	5015	99.96	–	0
Side-chain				
Asn	–	0	–	0
Gln	1	0.02	–	0
Arg	1	0.02	–	0
His	–	0	1719	34.26
Phe	–	0	633	12.62
Trp	–	0	1461	29.12
Tyr	–	0	1204	24.00
Total	5017	100	5017	100

[a]The number of times a particular amino acid occurs in an appropriate interaction; [b]percent of amino acid occurs in an appropriate interaction

A typical interface with some of the amide–π interactions involving backbone planar residues (A:Ile36:C,O;Met37:N–A:His40) and side-chain residues (A:Gln14:N–A:Tyr16) is shown in Fig. 3a and b, respectively.

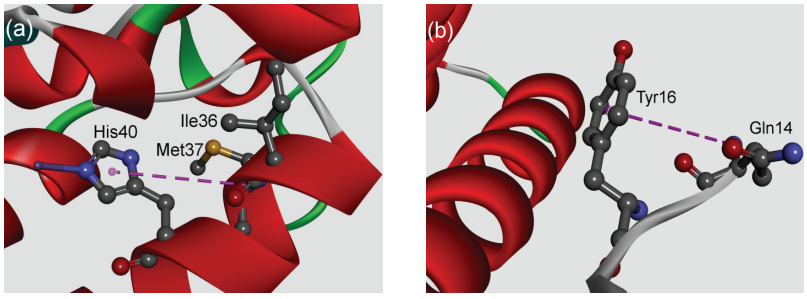

Fig. 3. Assorted examples of amide–π interactions for the MnSOD from *Aspergillus fumigatus* (PDB code 1kkc); a) backbone amide–π interaction, b) side-chain amide–π interaction. The interactions are marked with pink dashed lines.

The analysis showed that around 70 % of the total interacting residues in the dataset are involved in the formation of multiple amide–π interactions. In many

crystal structures of superoxide dismutases it is shown that a backbone amide is capable of binding with several aromatic residues. This type of interaction is marked as furcation. An illustrative example of amide–π interactions involving the presence of three aromatic groups surrounding one backbone amide is shown in Fig. 4. A backbone amide group from A:Met37–Glu38 can interact with three aromatic rings of A:His40, His42 and Trp92 simultaneously. This emphasizes the previous findings that furcation is an inherent characteristic of the superoxide dismutase.[29] The importance of multiple non-covalent weak interactions for the cooperativity and the governing of the multicomponent supramolecular assemblies has been already reported.[45] The another additional feature is the observed additive property of these interactions, showing an effect on the strength of the host–guest system.

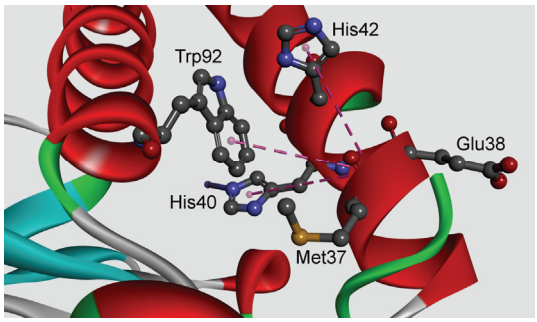

Fig. 4. Example of a multiple amide–π interaction for the MnSOD from *Aspergillus fumigatus* (PDB code 1kkc); the interactions are marked with dashed lines.

Interaction geometries and energetic contribution of amide–π interactions

The frequency distribution of the distance and the angle parameters of amide––π interaction pairs were analyzed (Fig. 5). The distribution of R_{cen}, the centroid––centroid distance, for the amide–π interactions was found to be in the rather broad range of 4.5–7.0 Å (Fig. 5a), without showing a clear geometrical preference. However, a small number of interactions also occurs at distances below 4.5 Å, indicating an attractive interaction. A distribution of the R_{clo} distances shows a clear maxima of about 5 Å. This is in accordance with the centroid distances. The majority of furcated interactions exhibit longer distances than the simple non-furcated interactions, as expected.[29] The native structure represents the compromise of a large number of noncovalent interactions existing in proteins. The geometrical features relating two residue-types are expected to be rather broad.

The aromatic ring–amide angles were distributed between full range (0–90° range), with a preference for higher angle values (Fig. 5d). A distribution of the angles below 30° shows coplanarity, possibly due to the maximizing amide–π stacking and packing,[46] while the axial aromatic–amide pairs are more likely to have T-shaped orientation s(γ> 60°). In general, as the distance of the backbone amide from the aromatic residue increases, the occurrence of perpendicular

orientations increased as well. Values of the θ angle (Fig. 5c) were in good agreement with distributions of aromatic ring–amide angles. The freedom of rotation of the aromatic ring is restricted, whereas the rotamer distributions usually depend on the backbone conformation. There is no significant statistical difference in the γ angle distribution between the multiple and the single amide–π interactions. The preferred orientations are quite similar to those found in aromatic–aromatic interactions,[47] and T-shaped orientation is observed. In the parallel-stacked case, van der Waals contribution is the dominant effect and the electrostatics contribution is actually repulsive, although small in value (<1 kcal mol^{-1}). On the other hand, the van der Waals contribution in the T-shaped case is not overwhelming, and it is the attractive electrostatics contribution that results in the overall binding of ~2.0 kcal mol^{-1}.[7,46]

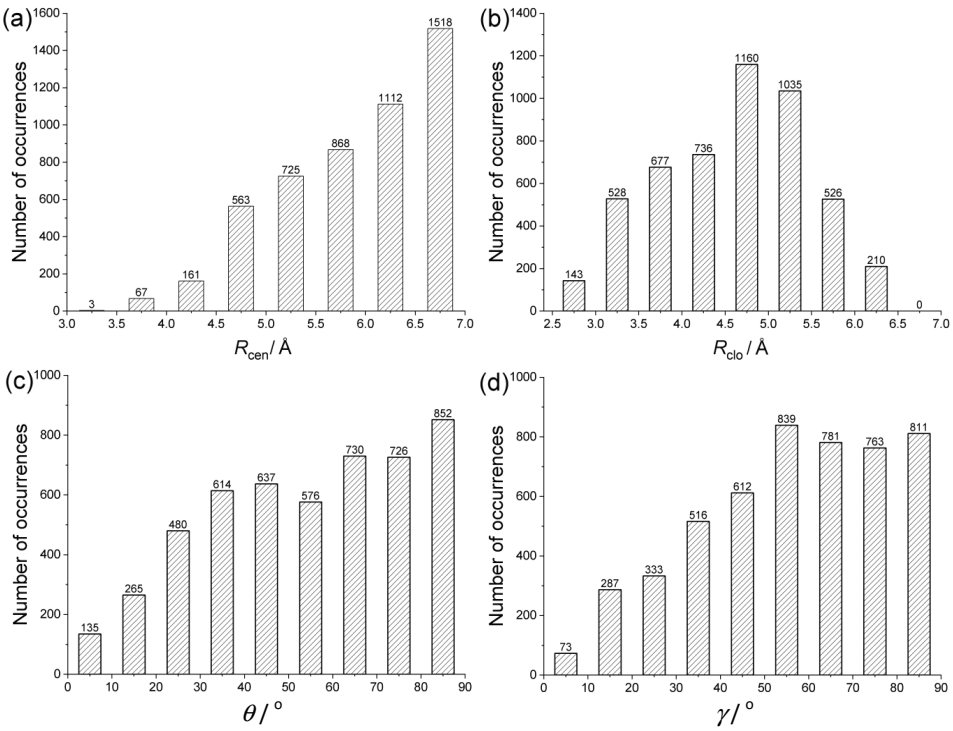

Fig. 5. Interaction geometries of amide–π interactions: a) R_{cen} distance distribution, b) R_{clo} distance distribution, c) θ angle distribution, d) γ angle distribution.

To estimate the stabilization energy of the different amide–π pairs, the energy calculations were carried out. To avoid the calculation of more than 5000 interactions, 150 structures were selected and they represent almost all of the interactions which had been found. In our database we found that the amide–π interactions energy is lower than –7 kcal mol^{-1}, and most of them have energy in the

range –1 to –4 kcal mol^{-1} (Fig. 6). The energies of the weakly polar amide–π interactions examined here are in the lower range of strong hydrogen bonds (–4 to –15 kcal mol^{-1}), as classified by Desiraju and Steiner.[48] Thus, the amide–π interactions make a substantial impact on the conformational stability of proteins. The energy of the interaction between the aromatic ring backbone amide has a complex dependence on side chain rotamer orientations and the dynamics of the backbone.

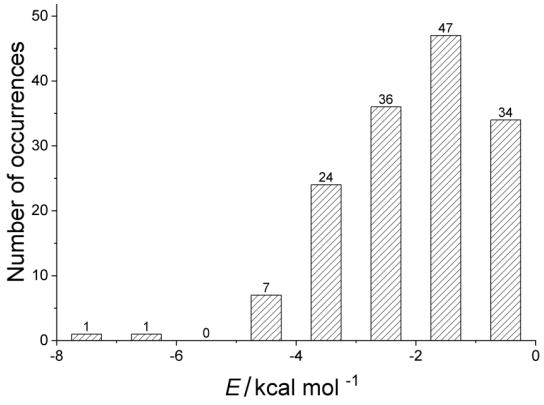

Fig. 6. Interaction energies of amide–π interactions.

Fig. 7 shows the preferred amide–π interactions of FeSOD from the thermophilic cyanobacterium *Thermosynechococcus elongatus.*

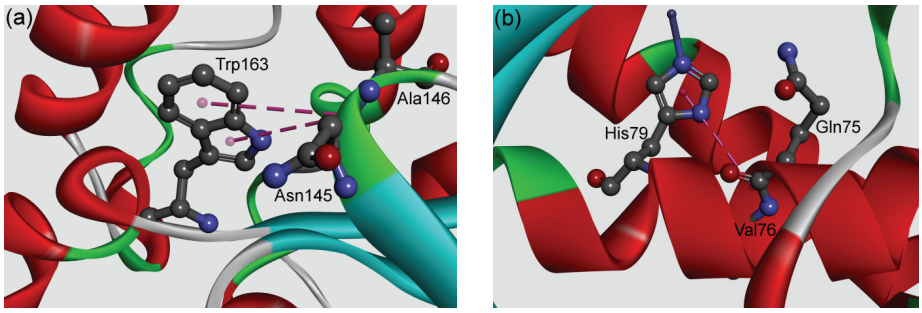

Fig. 7. Example of the structure preferred amide–π interactions of FeSOD from the *Thermosynechococcus elongatus* (PDB code 1my6): a) parallel-displaced and b) T-shaped structure. The interactions are marked with dashed lines.

The results of our *ab initio* calculations of optimized structures showed that the strongest attractive amide–π interactions exists in two preferred intermolecular structures, parallel-dis¬placed (A:Asn145:C,O;Ala146:N—A:Trp163; E = –7.05 kcal mol^{-1}; R_{cen} = 4.8 Å; R_{clo} = 2.9 Å) and T-shaped structures (A:Gln75:C,O;Val76:N A:His79; E = −6.89 kcal mol^{-1}; R_{cen} = 4.8 Å; R_{clo} = 2.8 Å).

Stabilization centres and conservation of amino acid residues

Stabilization centres (SC) are composed of certain clusters of residues, involved in the cooperative long range interaction of proteins that regulate flexibility, rigidity and stability of the protein structures. The most frequent stabilization centre residues are usually found at buried positions and have hydrophobic or aromatic side-chains, but some polar or charged residues may also play an important role in stabilization. The stabilization centres, when compared with the rest of the residues, showed a significant difference in the composition and in the type of the linked secondary structural elements. The performed structural and sequential conservation analysis showed a higher conservation of stabilization centres over protein families.[40] The stabilization centres for all amide–π interaction forming residues in SOD active centres were computed. Considering the whole data set, 39.6 % of all stabilizing residues are involved in building the amide–π interactions. It is interesting to note that all the residues involved in amide–π interactions were included in at least one stabilization centre. These observations strongly suggest that those residues may contribute significantly to the structural stability of the studied proteins in addition to participating in amide–π interactions.

From the presented analysis, it was found that more than 69 % of amide–π interacting residues in SOD were highly conserved, with a score ≥6, revealing their importance in the stability of protein structure.

CONCLUSION

The influence of amide–π interactions on the stability of SOD active centres was analysed in this research. It was found that most of the interactions occurs in the backbone of proteins. From the results it can be underlined that around 70 % of the total interacting residues in the dataset were involved in the formation of the multiple amide–π interactions. The distribution of distances for the amide–π interactions was found to be in the rather broad range of 4.5–7.0 Å, without clear geometrical preference. The amide–π interactions exists mainly in two preferred geometries, parallel-displaced and T-shaped structures. There is no significant statistical difference in the distances and the angle distribution between the multiple and the single amide–π interactions. the results suggested that the majority of the amide–π interactions showed some energy mostly in the range –1 to –4 kcal mol^{-1}. Moreover, the majority of the residues involved in amide–π interactions were evolutionarily conserved; all residues involved in amide–π interactions are included in at least one stabilization centre, thus providing an additional stabilization of the SOD proteins. The quantification of such interactions is of great importance for a rational approach to the biological systems including their protein structure and function, as well as for the further development of drug design processes.

Acknowledgement. The authors would like to thank the Ministry of Education, Science and Technological Development of Republic of Serbia (Grants No: 451-03-9/2021--14/200026, 451-03-9/2021-14/200104 and 451-03-9/2021-14/200168) for financial support.

ИЗВОД

АМИД–π ИНТЕРАКЦИЈЕ У АКТИВНОМ ЦЕНТРУ СУПЕРОКСИД-ДИСМУТАЗА

СРЂАН Ђ. СТОЈАНОВИЋ[1], ЗОРАН З. ПЕТРОВИЋ[2] и МАРИО В. ЗЛАТОВИЋ[3]

[1]Универзитет у Београду-Институт за хемију, технологију и металургију, Београд, [2]Математички факултет, Универзитет у Београду, Београд и [3]Хемијски факултет, Универзитет у Београду, Београд

У овом раду је анализиран утицај амид–π интеракција на стабилност и особине активног центра супероксид-дисмутазе (SOD). Примећено је 5017 амид–π интеракција у сету података од 43 протеина, где, просечно, сваки активни центар формира 117 интеракција. Већина интеракција је укључена у основни ланац протеина. Анализа геометрије амид–π интеракција открива две приоритетне структуре, паралелно-измештен (*parallel--displaced*) и Т-облик (T-*shaped*) структуре. Ова студија има за циљ истраживање доприноса енергије амид–π интеракција чије јачине су у доњем рангу јаких водоничних веза. Преглед конзервираности показује да је више од половине остатака укључених у ове интеракције еволутивно конзервирано. Стабилизациони центри ових протеина показују да су сви остаци који чине амид– интеракције важни у распоређивању једног или више таквих центара. Свеукупно, резултати у овом раду ће бити врло корисни за разумевање доприноса амид–π интеракција када се анализира стабилност активних центара SOD.

(Примљено 21. марта, ревидирано 1. јуна, прихваћено 2. јуна 2021)

REFERENCES

1. E. A. Meyer, R. K. Castellano, F. Diederich, *Angew. Chem., Int. Ed. Engl*. **42** (2003) 1210 (https://doi.org/10.1002/anie.200390319)
2. L. M. Salonen, M. Ellermann, F. Diederich, *Angew. Chem., Int. Ed. Engl*. **50** (2011) 4808 (https://doi.org/10.1002/anie.201007560)
3. N. Acharjee, *J. Serb. Chem. Soc*. **85** (2020) 765 (https://doi.org/10.2298/JSC190914136A)
4. M. Levitt, M. F. Perutz, *J. Mol. Biol*. **201** (1988) 751 (https://doi.org/10.1016/0022-2836(88)90471-8)
5. J. Cheney, B. V. Cheney, W. G. Richards, *Biochim. Biophys. Acta* **954** (1988) 137 (https://doi.org/10.1016/0167-4838(88)90063-5)
6. G. Duan, V. H. Smith, D. F. Weaver, *Chem. Phys. Lett.* **310** (1999) 323 (https://doi.org/10.1016/S0009-2614(99)00804-0)
7. M. Harder, B. Kuhn, F. Diederich, *ChemMedChem* **8** (2013) 397 (https://doi.org/10.1002/cmdc.201200512)
8. S. Cotesta, M. Stahl, *J. Mol. Model*. **12** (2006) 436 (https://doi.org/10.1007/s00894-005-0067-x)
9. S. K. Burley, G. A. Petsko, *Science* **229** (1985) 23 (https://doi.org/10.1126/science.3892686)
10. S. K. Burley, G. A. Petsko, *FEBS Lett*. **203** (1986) 139 (https://doi.org/10.1016/0014-5793(86)80730-x)

11. S. K. Burley, G. A. Petsko, *Adv. Protein Chem*. **39** (1988) 125 (https://doi.org/10.1016/s0065-3233(08)60376-9)
12. T. Steiner, G. Koellner, *J. Mol. Biol*. **305** (2001) 535 (https://doi.org/10.1006/jmbi.2000.4301)
13. F. R. Ferreira de, M. Schapira, *MedChemComm* **8** (2017) 1970 (https://doi.org/10.1039/c7md00381a)
14. M. Giroud, J. Ivkovic, M. Martignoni, M. Fleuti, N. Trapp, W. Haap, A. Kuglstatter, J. Benz, B. Kuhn, T. Schirmeister, F. Diederich, *ChemMedChem* **12** (2017) 257 (https://doi.org/10.1002/cmdc.201600563)
15. S. Raghunathan, T. Jaganade, U. D. Priyakumar, *Biophys. Rev*. **12** (2020) 65 (https://doi.org/10.1007/s12551-020-00620-9)
16. M. Giroud, M. Harder, B. Kuhn, W. Haap, N. Trapp, W. B. Schweizer, T. Schirmeister, F. Diederich, *ChemMedChem* **11** (2016) 1042 (https://doi.org/10.1002/cmdc.201600132)
17. L. M. Salonen, M. C. Holland, P. S. Kaib, W. Haap, J. Benz, J. L. Mary, O. Kuster, W. B. Schweizer, D. W. Banner, F. Diederich, *Chemistry* **18** (2012) 213 (https://doi.org/10.1002/chem.201102571)
18. B. S. Lauber, L. A. Hardegger, K. A. Alam, B. A. Lund, O. Dumele, M. Harder, B. Kuhn, R. A. Engh, F. Diederich, *Chemistry* **22** (2016) 211 (https://doi.org/10.1002/chem.201503552)
19. V. Ehmke, E. Winkler, D. W. Banner, W. Haap, W. B. Schweizer, M. Rottmann, M. Kaiser, C. Freymond, T. Schirmeister, F. Diederich, *ChemMedChem* **8** (2013) 967 (https://doi.org/10.1002/cmdc.201300112)
20. G. R. De, E. Brodbeck-Persch, S. Bryson, N. B. Hentzen, M. Kaiser, E. F. Pai, R. L. Krauth-Siegel, F. Diederich, *ChemMedChem* **13** (2018) 957 (https://doi.org/10.1002/cmdc.201800067)
21. M. W. Krone, C. R. Travis, G. Y. Lee, H. J. Eckvahl, K. N. Houk, M. L. Waters, *J. Am. Chem. Soc*. **142** (2020) 17048 (https://doi.org/10.1021/jacs.0c06568)
22. K. DeFrees, M. T. Kemp, X. ElHilali-Pollard, X. Zhang, A. Mohamed, Y. Chen, A. R. Renslo, *Org. Chem. Front*. **6** (2019) 1749 (https://doi.org/10.1039/c9qo00342h)
23. R. Meurisse, R. Brasseur, A. Thomas, *Proteins* **54** (2004) 478 (https://doi.org/10.1002/prot.10582)
24. P. W. Rose, B. Beran, C. Bi, W. F. Bluhm, D. Dimitropoulos, D. S. Goodsell, A. Prlic, M. Quesada, G. B. Quinn, J. D. Westbrook, J. Young, B. Yukich, C. Zardecki, H. M. Berman, P. E. Bourne, *Nucleic Acids Res*. **39** (2011) D392 (https://doi.org/10.1093/nar/gkq1021)
25. J. M. Word, S. C. Lovell, J. S. Richardson, D. C. Richardson, *J. Mol. Biol*. **285** (1999) 1735 (https://doi.org/10.1006/jmbi.1998.2401)
26. *Accelrys Software Inc., Discovery Studio Visualizer, Release 2020*, Accelrys Software Inc., San Diego, CA, 2020
27. M. R. Jackson, R. Beahm, S. Duvvuru, C. Narasimhan, J. Wu, H. N. Wang, V. M. Philip, R. J. Hinde, E. E. Howell, *J. Phys. Chem., B* **111** (2007) 8242 (https://doi.org/10.1021/jp0661995)
28. V. Philip, J. Harris, R. Adams, D. Nguyen, J. Spiers, J. Baudry, E. E. Howell, R. J. Hinde, *Biochemistry* **50** (2011) 2939 (https://doi.org/10.1021/bi200066k)
29. V. R. Ribić, S. Đ. Stojanović, M. V. Zlatović, *Int. J. Biol. Macromol*. **106** (2018) 559 (https://doi.org/10.1016/j.ijbiomac.2017.08.050)

30. J. Hostaš, D. Jakubec, R. A. Laskowski, R. Gnanasekaran, J. Řezáč, J. Vondrášek, P. Hobza, *J. Chem. Theory Comput.* **11** (2015) 4086 (http://dx.doi.org/10.1021/acs.jctc.5b00398)
31. *Schrödinger Release 2018-1, Jaguar, Schrödinger*, LLC, New York, NY, 2018
32. T. H. Dunning, *J. Chem. Phys*. **90** (1989) 1007 (https://doi.org/10.1063/1.456153)
33. T. Clark, J. Chandrasekhar, G. n. W. Spitznagel, P. V. R. Schleyer, *J. Comput. Chem.* **4** (1983) 294 (https://doi.org/10.1002/jcc.540040303)
34. A. D. Bochevarov, E. Harder, T. F. Hughes, J. R. Greenwood, D. A. Braden, D. M. Philipp, D. Rinaldo, M. D. Halls, J. Zhang, R. A. Friesner, *Int. J. Quantum Chem*. **113** (2013) 2110 (https://doi.org/10.1002/qua.24481)
35. G. J. Jones, A. Robertazzi, J. A. Platts, *J. Phys. Chem., B* **117** (2013) 3315 (https://doi.org/10.1021/jp400345s)
36. K. E. Riley, J. A. Platts, J. Řezáč, P. Hobza, J. G. Hill, *J. Phys. Chem., A* **116** (2012) 4159 (https://doi.org/10.1021/jp211997b)
37. S. Saebø, W. Tong, P. Pulay, *J. Chem. Phys.* **98** (1993) 2170 (https://doi.org/10.1063/1.464195)
38. A. Reyes, L. Fomina, L. Rumsh, S. Fomine, *Int. J. Quantum Chem.* **104** (2005) 335 (https://doi.org/10.1002/qua.20558)
39. R. M. Balabin, *J. Chem. Phys.* **132** (2010) 231101 (https://doi.org/10.1063/1.3442466)
40. Z. Dosztányi, A. Fiser, I. Simon, *J. Mol. Biol*. **272** (1997) 597 (https://doi.org/10.1006/jmbi.1997.1242)
41. Z. Dosztányi, C. Magyar, G. Tusnady, I. Simon, *Bioinformatics* **19** (2003) 899 (https://doi.org/10.1093/bioinformatics/btg110)
42. H. Ashkenazy, E. Erez, E. Martz, T. Pupko, N. Ben-Tal, *Nucleic Acids Res.* **38** (2010) W529 (https://doi.org/10.1093/nar/gkq399)
43. B. Boeckmann, A. Bairoch, R. Apweiler, M. C. Blatter, A. Estreicher, E. Gasteiger, M. J. Martin, K. Michoud, C. O'Donovan, I. Phan, S. Pilbout, M. Schneider, *Nucleic Acids Res*. **31** (2003) 365 (https://doi.org/10.1093/nar/gkg095)
44. G. Toth, C. R. Watts, R. F. Murphy, S. Lovas, *Proteins* **43** (2001) 373 (https://doi.org/10.1002/prot.1050)
45. A. S. Mahadevi, G. N. Sastry, *Chem. Rev*. **116** (2016) 2775 (https://doi.org/10.1021/cr500344e)
46. G. B. McGaughey, M. Gagne, A. K. Rappe, *J. Biol. Chem*. **273** (1998) 15458 (https://doi.org/10.1074/jbc.273.25.15458)
47. B. P. Dimitrijević, S. Z. Borozan, S. Đ. Stojanović, *RSC Adv*. **2** (2012) 12963 (https://doi.org/10.1039/C2RA21937A)
48. G. R. Desiraju, T. Steiner, *The Weak Hydrogen Bond*, Oxford University Press, Oxford, 1999.